Lee and Han *Int J Concr Struct Mater* (2021) 15:5
https://doi.org/10.1186/s40069-020-00446-5

International Journal of Concrete Structures and Materials

RESEARCH Open Access

An Accurate Numerical Model Simulating Hysteretic Behavior of Reinforced Concrete Columns Irrespective of Types of Loading Protocols

Chang Seok Lee and Sang Whan Han*

Abstract

In older reinforced concrete (RC) buildings, columns are fragile elements that can induce collapse of entire buildings during earthquakes. An accurate assessment of the seismic vulnerability of RC buildings using nonlinear response history analyses requires an accurate numerical model. The peak-oriented hysteretic rule is often used in existing numerical models to simulate the hysteretic behavior of RC members, with predefined backbone curves and cyclic deterioration. A monotonic backbone curve is commonly constructed from a cyclic envelope. Because cyclic envelope varies according to loading protocols, particularly in a softening branch, it is difficult to obtain a unique backbone curve irrespective of loading protocols. In addition, cyclic deterioration parameters irrespective of loading protocols cannot be found because these parameters are estimated with respect to the backbone curves. Modeling parameters of existing numerical models can also vary with respect to loading protocol. The objective of this study is to propose a loading protocol-independent numerical model that does not require estimates of modeling parameters specifically tuned for a certain loading protocol. The accuracy of the proposed model is verified by comparing the simulated and measured cyclic curves of different sets of identical RC column specimens under various loading protocols.

Keywords: numerical model, column, loading protocol, cyclic envelope, backbone curve, peak oriented, cyclic deterioration

1 Introduction

Many older reinforced concrete (RC) buildings were built without considering important seismic design principles (Galanis and Moehle, 2015; Han et al. 2004; Moon et al. 2017; Sezen and Chowdhury 2009; Sae-Long et al. 2019). Columns in these buildings were often constructed with less-stringent reinforcement details than those required by modern seismic design codes (Lynn et al. 1996; Li and Sanada 2017; Chowdhury and Orakcal 2012; El-Sokkary and Galal 2009; Sezen and Moehle 2006; Elwood and Moehle 2005; Liel et al. 2011), making them vulnerable to earthquakes (Lee and Han 2018). Previous studies revealed that columns in RC buildings constructed prior to the 1970s exhibited poor hysteretic behavior (Galanis and Moehle 2015; Sezen and Chowdhury 2009), which can trigger partial or entire building collapse during earthquakes (Liel et al. 2011; Lee and Han 2018).

To assess the seismic vulnerability of such buildings and prepare adequate seismic retrofit plans using nonlinear response history analyses, it is necessary to employ an accurate numerical model. Numerical models have been developed to predict the hysteretic behavior of RC columns (Ghannoum and Moehle 2012; LeBorgne and Ghannoum 2014a, b). Such models are typically classified as lumped, distributed and continuum inelasticity

*Correspondence: swhan82@gmail.com
Department of Architectural Engineering, Hanyang University, Seoul 04763, Korea
Journal information: ISSN1976-0485 / eISSN 2234-1315

models (ATC 2010; NIST 2010; Ronagh and Baji 2014). Because of simplicity and efficiency, a lumped inelasticity model has been widely used (Haselton et al. 2011; Lignos et al. 2015, 2013; Elkady and Lignos 2014; Eads et al. 2013; Tothong, and Luco 2007; Goulet et al. 2007). In the lumped inelasticity model, a column is modeled using an elastic linear element and inelastic spring elements lumped at the both ends of the linear element. This model can effectively capture monotonic (in-cycle) and cyclic strength degradation of RC columns (ATC 2010).

In lumped inelasticity models recently developed for RC columns (Ibarra et al 2005; Lignos and Krawinkler 2011; Lowes and Altoontash 2003), the hysteretic rule, backbone curve, and damage rule must be defined. In the existing numerical models, monotonic and cyclic strength degradation are incorporated in the backbone curve and damage rule, respectively (Lowes and Altoontash 2003). Most existing numerical models for RC members (Haselton et al. 2007; Wen et al. 1996; LeBorgne and Ghannoum 2014a, b) commonly adopt the peak-oriented hysteretic rule proposed by Clough and Johnston (1966) and Mahin and Bertero (1976).

The procedure determining constituent modeling parameters of backbone curves and damage rule, however, varies from researcher to researcher, and relies heavily on measured cyclic curves of RC columns. Ideally, backbone curve parameters should be determined from monotonic tests, which have rarely been conducted. For this reason, most studies derived backbone curve parameters from the first-cycle envelopes of cyclic curves generated by experimental tests (FEMA 2009). However, there are two drawbacks in such procedure. First, at a given drift, the backbone curve derived from the first-cycle envelope generally produces a lateral load less than that from the monotonic tests, so that it produces conservative load–deformation responses (ASCE 2017). Second, the deformation at the peak load and the slope of softening branch in the first-cycle envelopes vary significantly according to loading protocols (FEMA 2009; ASCE 2017; Park and Ang 1985), making it impossible to obtain a unique backbone curve from the first-cycle envelope curve irrespective of loading protocols.

To reduce the uncertainties in the first-cycle envelopes, ASCE 41-17 (ASCE 2017) recommends that backbone curves be constructed using the median of multiple first-cycle envelopes obtained under different loading protocols. However, the ASCE 41-17 procedure may not be practical because most column specimens are tested under a single loading protocol rather than multiple loading protocols. A numerical model with an inaccurate backbone curve reportedly failed to accurately predict the collapse strength of a building when monotonic strength degradation played an important role in dynamic instability (Maison and Speicher 2016; PEER 2017). In addition, the modeling parameters of cyclic degradation cannot be estimated accurately because cyclic degradation is defined with respect to backbone curves.

The objective of this study is to propose a loading protocol-independent numerical model to tackle the aforementioned drawbacks. A backbone curve without a softening branch is used to idealize the backbone curve such that the influence of loading protocols on backbone curve idealization is minimized. A damage rule used in the proposed model can represent both monotonic and cyclic strength degradation. Unlike existing models, the proposed model does not require repeated estimations of modeling parameters according to loading protocols. The proposed numerical model is verified by comparing the simulated and measured cyclic curves of four sets of RC column specimens. Each set includes identical specimens tested under different loading protocols.

1.1 Exploration on the Effect of Different Loading Protocols on Envelope Curves

To explore the effect of different loading protocols on envelope curves, four sets of RC column tests are collected: (1) two specimens tested by Sezen and Moehle (2006); (2) six specimens tested by Takemura and Kawashima (1997); (3) five specimens tested by Nojavan et al. (2015), and (4) four specimens tested by Pujol et al. (2006). Each set contains RC column specimens with identical dimensions and reinforcement details, but the specimens in each set were tested under different loading protocols.

Table 1 summarizes information about collected specimens, where b is the width of a column section, h is the height of a column section, s is the center-to-center spacing of transverse reinforcement, a_v is the shear span, f_c' is the compressive strength of concrete, f_{yl} is the yield strength of the longitudinal reinforcement, f_{yt} is the yield strength of the transverse reinforcement, ρ_l is the ratio of area of distributed longitudinal reinforcement to gross concrete area perpendicular to that reinforcement, and ρ_t is the ratio of area of distributed transverse reinforcement to gross concrete area perpendicular to that reinforcement.

In Table 1, "MONO", "STD", "OS", and "CA" indicate monotonic loading, fully reversed cyclic loading with gradually increasing deformation amplitudes, one-sided loading, and cyclic loading with constant displacement amplitude, respectively. Some specimens (S2, T4, N3, N4, and N5) listed in Table 1 were tested under mixed loading protocols. For example, specimen S2 was tested under loading protocol STD in the initial loading phase,

Table 1 Summary of physical parameters of RC column specimens and loading protocols.

Set	ID	b (mm)	h (mm)	a_v (mm)	v (%)	f'_c (MPa)	f_{yl} (MPa)	ρ_l (%)	ρ_t (%)	Loading protocol	References
1	S1	457	457	1473	15.1	21.1	434	2.48	0.17	STD	Sezen and Moehle (2006)
	S2	457	457	1473	14.6	21.8	434	2.48	0.17	STD + MONO	
2	T1	400	400	1245	2.7	35.9	363	1.58	0.20	STD	Takemura and Kawashima (1997)
	T2	400	400	1245	2.8	35.7	363	1.58	0.20	STD	
	T3	400	400	1245	2.9	34.3	363	1.58	0.20	STD	
	T4	400	400	1245	3.0	33.2	363	1.58	0.20	MONO + STD	
	T5	400	400	1245	2.7	36.8	363	1.58	0.20	OS	
	T6	400	400	1245	2.7	35.9	363	1.58	0.20	OS	
3	N1	914	711	1473	15.4	37.2	510	1.59	1.02	STD	Nojavan et al. (2015)
	N2	914	711	1473	13.9	33.5	510	1.59	1.02	MONO	
	N3	914	711	1473	14.1	36.5	510	1.59	1.02	STD + MONO	
	N4	914	711	1473	14.0	37.0	510	1.59	1.02	STD + MONO	
	N5	914	711	1473	16.3	31.8	510	1.59	1.02	STD + OS	
4	P1	152	305	686	9.6	29.9	453	2.45	0.55	CA	Pujol et al. (2006)
	P2	152	305	686	9.6	29.9	453	2.45	0.55	CA	
	P3	152	305	686	8.5	33.7	453	2.45	0.55	CA	
	P4	152	305	686	8.5	33.7	453	2.45	0.55	CA	

then under loading protocol MONO in a subsequent loading phase.

Figure 1a–d shows the first-cycle envelopes of three sets of column specimens in individual sets tested by Sezen and Moehle (2006), Takemura and Kawashima (1997), Nojavan et al. (2015), and Pujol et al. (2006), respectively. The abscissa and ordinate are the drift ratio (θ) and lateral load, respectively. Although specimens in each set had identical geometrical properties, the first-cycle envelopes vary significantly from specimen-to-specimen because of the influence of different loading protocols (see Fig. 1a–c). Specimens tested under loading protocol STD generally have the smallest first-cycle envelope compared with specimens tested under other loading protocols (MONO and OS). This phenomenon agrees with that reported by previous studies (FEMA 2009; ASCE 2017; Park and Ang 1985).

According to Sezen and Moehle (2006), Takemura and Kawashima (1997), and Nojavan et al. (2015), all specimens experienced reinforcement yielding at θ ranging from 1 to 2%, a relatively narrow range. As shown in Fig. 2, the variability of the first-cycle envelopes is not significant in the elastic range. However, as θ increases beyond the elastic range, variability in envelopes according to loading protocols grows sharply. In Fig. 1, median ($\hat{X}$) and $\hat{X} \pm$ one standard deviation (σ) of envelopes are plotted. The $\hat{X} \pm \sigma$ envelope deviates more from corresponding $\hat{X}$ envelopes with an increase in θ. This phenomenon is more evident beyond the linear-elastic range. The first-cycle envelopes shown in Fig. 1d did not exhibit large dispersions (σ). This may be attributed to two reasons: (1) displacement amplitudes used in tests were not large enough for reaching capping point; (2) tests were conducted with relatively simple and symmetric loading protocols.

Figure 2 depicts the backbone curves derived from the envelopes by Haselton et al. (2007). Two sets of column tests conducted by Sezen and Moehle (2006), Takemura and Kawashima (1997) are considered. Although the backbone curves of identical specimens should be the same irrespective of loading protocols, backbone curves obtained from cyclic envelopes vary significantly.

Large variation is also observed in capping deformation (θ at maximum load). As shown in Fig. 2b, the effective yield points (θ_y) of individual specimens are less than 2%. Beyond θ_y, the stiffness of backbone curves decreases significantly. Because cyclic strength degradation is defined with respect to the backbone curves, the values of modeling parameters for cyclic degradation also vary significantly according to loading protocols. The difference in values of cyclic degradation parameters estimated by Haselton et al. (2007) for specimens T1 and T5 is as large as 364%.

To obtain a unique set of backbone curves and cyclic degradation irrespective of loading protocols, experimental tests are required with a number of identical specimens under monotonic loading as well as various cyclic loading protocols. Krawinkler (2009) mentioned an urgent need to complement conventional component tests, which are usually based on gradually increasing symmetric loading protocols. However, conducting such experimental tests require enormous efforts and time.

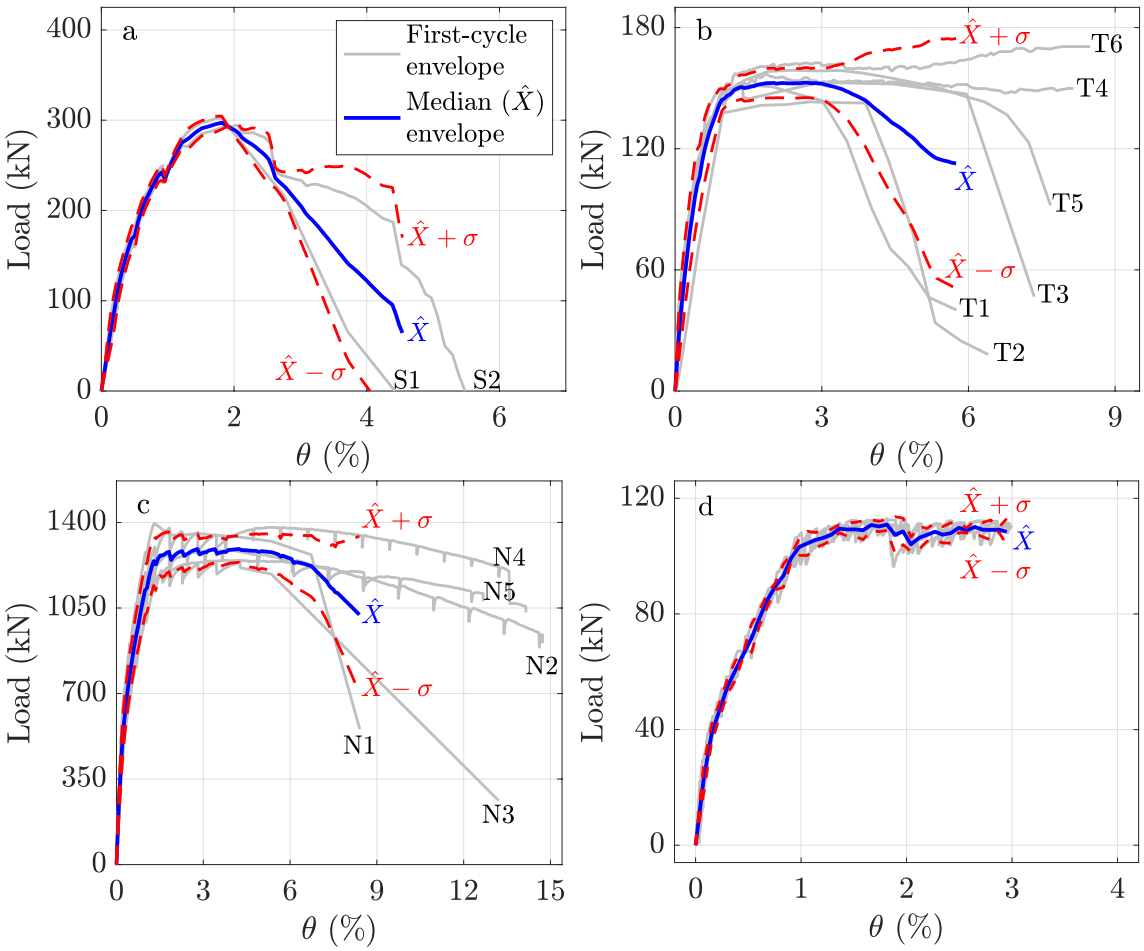

Fig. 1 Cyclic envelopes of three sets of identical RC specimens tested under various loading protocols: **a** Sezen and Moehle (2006), **b** Takemura and Kawashima (1997), **c** Nojavan et al. (2015), **d** Pujol et al. (2006).

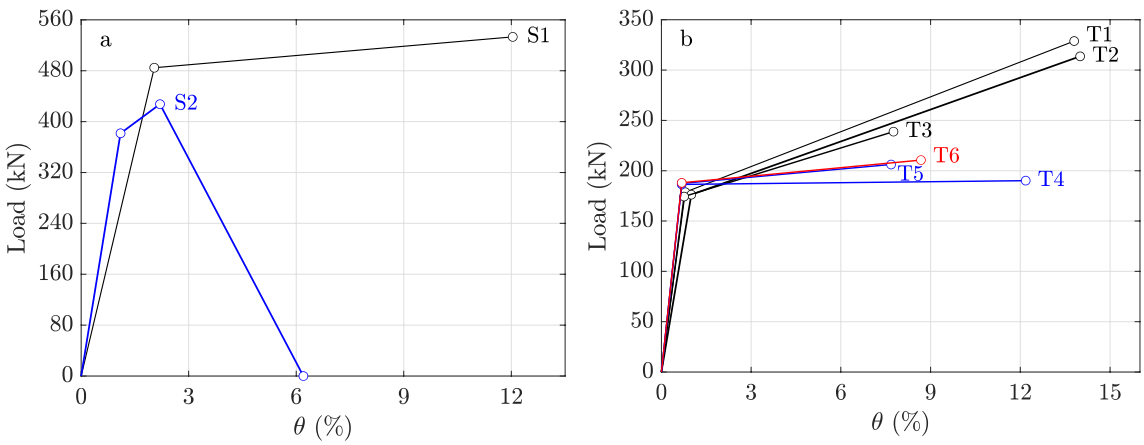

Fig. 2 Backbone curves idealized from cyclic envelopes for different loading protocols: **a** Sezen and Moehle (2006), **b** Takemura and Kawashima (1997).

2 Numerical Model Proposed for RC Columns in This Study

A loading protocol-independent numerical model is proposed to simulate the hysteretic behavior of RC columns in this study. Although the proposed model is developed based on the peak-oriented hysteretic rule, there are two distinct differences from the existing models: (1) a softening branch is not included in the backbone curves, and (2) a damage rule that accommodates both monotonic and cyclic strength degradation is used. A more detailed explanation of the proposed model follows.

2.1 Backbone Curve and Hysteretic Rule

In existing numerical models, backbone curves are typically defined prior to simulating cyclic curves (Ibarra et al. 2005; Lows and Altoontash 2003). Tri-linear backbone curves are most often used in numerical models for RC columns (Haselton et al. 2007): (1) the first line segment of the backbone curves starts from the origin to the effective yield point, which represents the elastic response of RC columns; (2) the second line segment connecting the effective yield and capping (maximum load) points represents strain hardening behavior, and (3) the third line segment is a softening branch, which connects the capping and reduced-strength points and represents monotonic strength degradation.

In this study, a backbone curve without a softening branch beyond the capping point (θ_c, f_c) is used to avoid the loading protocol-dependent nature in softening branch (Fig. 3a). The softening branch varies widely according to loading protocols (Fig. 1). An additional advantage of using backbone curves without a softening branch is that fewer backbone curve parameters are needed by the numerical model. Although the softening branch is not included in the backbone curve, monotonic strength degradation is considered in the proposed model with a modified damage rule, described in the following section.

Most existing numerical models adopt the peak-oriented hysteretic rule to simulate the hysteretic behavior of RC structural components (Lows and Altoontash 2003; LeBorgne and Ghannoum 2014a, b). In this study, the peak-oriented hysteretic rule is also used in the proposed model. Peak-oriented hysteretic rules without and with pinching behavior are shown in Fig. 3 b and c, respectively. The pinching rule proposed by Lowes and Altoontash (2003) is also implemented in the proposed model (Fig. 3c). The pinched responses are simulated through break points (7′ and 8′ in Fig. 3c). The reloading break point is defined by the parameters κ_r and κ_d (Fig. 3c), which modifies the maximum pinched force and displacement (point 8′ in Fig. 3c), respectively. The reloading break points ($\kappa_r\theta_{max}$, $\kappa_d f_{max}$) in the positive and negative loading directions are defined with respect to maximum absolute values of force and deformation (θ_{max} and f_{max}). In the case of unloading break points (point 7′ in Fig. 3c), only the unloading force is modified as $\kappa_u f_c$. The values of pinching parameters (κ_r, κ_d and κ_u) are assigned between 0 and 1.

2.2 Damage Rule

During earthquakes, RC columns often experience micro-cracking, concrete spalling, concrete crushing, reinforcement yielding and bond deterioration at steel–concrete interfaces (Yue et al. 2016; Park and Paulay 1975). Degradation in strength (f) and stiffness (k) is a macroscopic representation of such damage. In existing numerical models, strength and stiffness degradation in the load–deformation responses is incorporated using Eq. (1):

$$x = (1 - \delta)\bar{x} \tag{1}$$

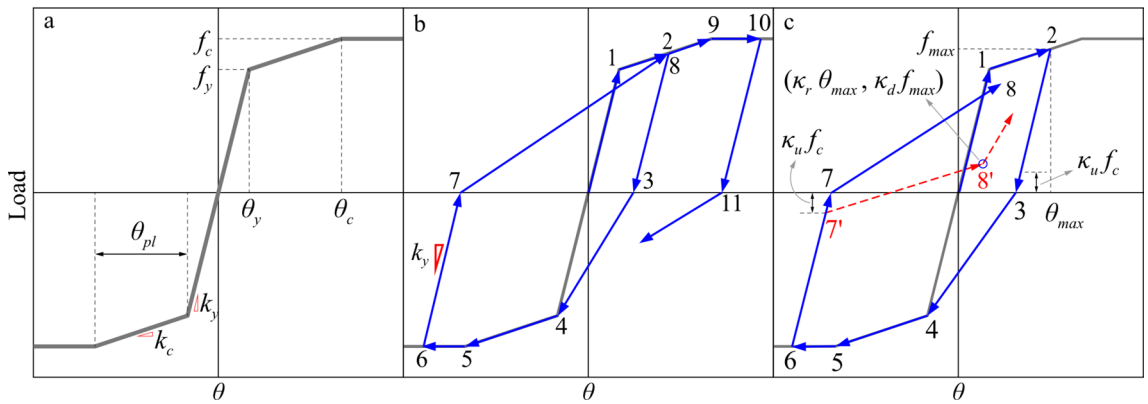

Fig. 3 Proposed numerical model: **a** backbone curve, **b** hysteretic rule without pinching, **c** hysteretic rule with pinching.

where $\bar{x}$ and x are the original and deteriorated response variables, respectively, and δ is the damage variable, which is equivalent to δ_i (Lowes and Altoontash 2003) and β_i (Ibarra et al. 2005; Lignos and Krawinker 2011). The role of a damage variable is to represent the degree of damage relative to the backbone curve. The value of δ varies between 0 and 1.

The damage variable δ in Eq. (1) can be calculated using Eq. (2):

$$\delta = \alpha_1 (D)^{\alpha_2} \tag{2}$$

where α_1 and α_2 are the damage parameters defining the rate of degradation (damage) at a given D, and D is the damage function that estimates either cumulative energy [Eq. (3)] or cumulative deformation [Eq. (4)]:

$$D = \sum f \Delta\theta \tag{3}$$

$$D = \sum |\Delta\theta| \tag{4}$$

To account for strength and stiffness degradation in load–deformation responses, Eq. (3) is often used (Lee and Han 2018; Ibarra et al. 2005; Lignos and Krawinker 2011; Lowes and Altoontash 2003; Haselton et al. 2007; LeBorgne and Ghannoum 2014a, b; Han et al. 2019).

However, Eq. (3) does not reflect trends in damage accumulation according to deformation demands. The degree of damage accumulation accelerates with an increase in deformation (θ) and number of cyclic deformation reversals on RC columns. LeBorgne and Ghannoum (2014a, b) reported that such phenomena are more apparent in RC columns that fail by shear.

Figure 4a provides an example of load–deformation responses simulated with Eq. (3) subjected to eight cycles of loading with the same deformation amplitude. Figure 4b shows a normalized D calculated from the cyclic curves in Fig. 4a. Normalized D is the D value at each loading cycle divided by the value at the last loading cycle. As shown in this figure, the degree of increment in normalized D calculated from Eq. (3) per cycle decreases with an increase in the number of cycles unlike the trend reported by LeBorgne and Ghannoum (2014a, b), whereas the degree of increment calculated from Eq. (4) is nearly constant. In this study, a cumulative deformation rule is used to estimate the degree of damage.

To evaluate the accuracy in damage function (D), test results of 133 rectangular RC column specimens exhibiting the damage variable (δ) value for strength degradation greater than or equal to 0.5 are collected from the PEER Structural Performance Database (Berry et al. 2004). To derive the relation between D and δ, linear and logarithmic δ values are plotted according to normalized D values in Fig. 5a and b, respectively, where D is calculated from Eq. (4). Damage variable δ can be estimated at each deformation reversal, which is calculated as the measured lateral load divided by the maximum lateral load. In Fig. 5, δ is denoted by black dots. Figure 5a and b shows a median $\hat{X}$ and standard deviation (σ) of δ and $\ln\delta$, respectively. The dispersion in $\ln\delta$ according to normalized D is less than that in δ. The mean squared error of δ_i and $\ln\delta_i$ measured from their respective medians are 0.70 and 0.56. Thus, damage function D is proposed as an exponential form rather than a linear form. The proposed equation is:

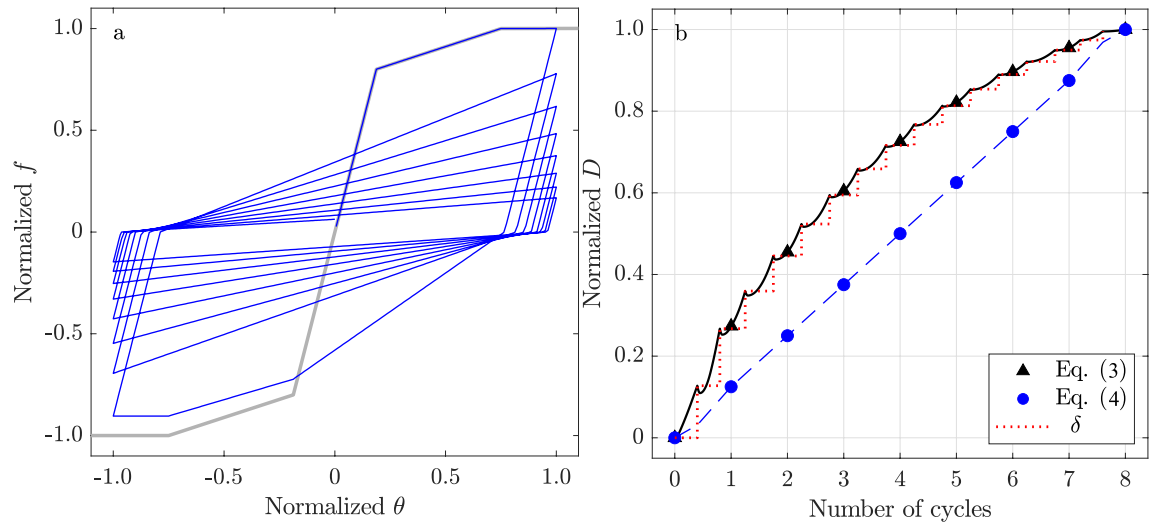

Fig. 4 Cyclic curves and damage accumulation: **a** cyclic curves, **b** normalized D per cycles.

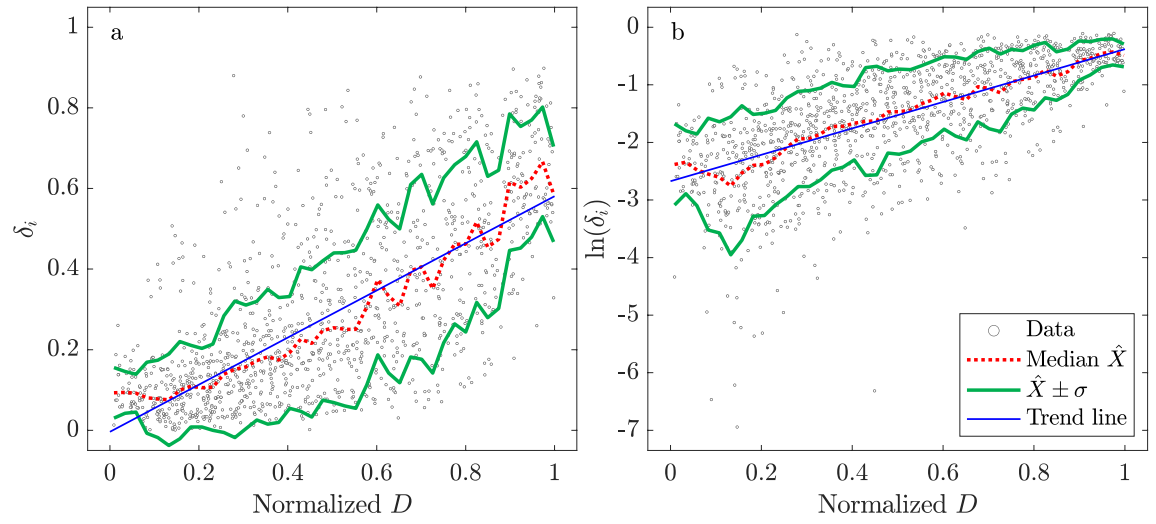

Fig. 5 Trend between δ_i and D.

$$D = \sum e^{|\theta-\theta_y|/\theta_{pl}}|\Delta\theta| \tag{5}$$

where $e^{|\theta-\theta_y|/\theta_{pl}}$ is the weight factor accounting for the trend between D and $\ln\delta$ as observed in Fig. 5b, and θ_{pl} is the plastic deformation defined in Fig. 3a.

In existing models (Lowes and Altoontash 2003; Ibarra et al 2005; Lignos and Krawinkler 2011), δ in Eq. (2) is updated at deformation reversals. This leads to an abrupt increase in δ, as denoted by the dotted line in Fig. 4b. In addition, monotonic strength degradation under a monotonically increasing load cannot be simulated by existing models. To introduce strength degradation under monotonic loading, a softening branch is included in a backbone curve in the existing models, which is difficult to predict because of the highly dependent nature of loading protocols (Fig. 1).

Such drawbacks can be alleviated by updating δ at every analysis step instead of updating it at deformation reversals. This updating scheme is based on softening-response prediction for concrete materials in continuum damage mechanics (Krajcinovic 1983). Figure 6a and b shows the load–deformation response

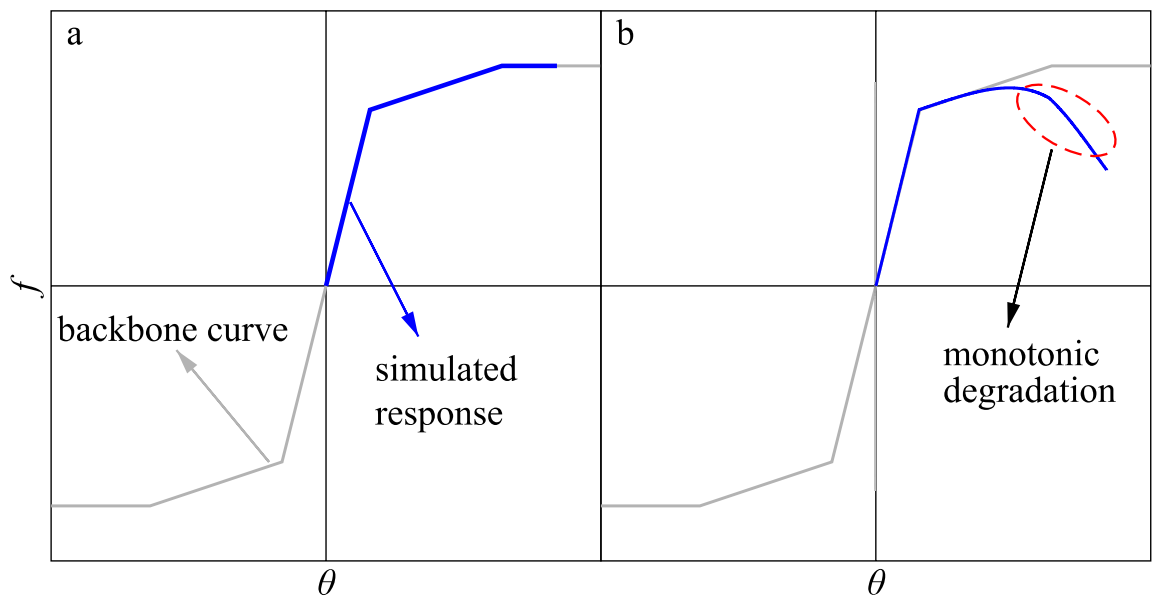

Fig. 6 Load–deformation response under monotonically increasing load: **a** existing model, **b** proposed model.

of existing and proposed models under monotonically increasing loading, respectively. Neither model includes a softening branch in the backbone curves to illustrate the novel feature of the proposed model. As shown in Fig. 6a, the existing model fails to simulate monotonic degradation when the softening branch is not defined in the backbone curve. The proposed model successfully simulates monotonic strength degradation, although a softening branch is not included in the backbone curve (Fig. 6b).

Figure 7 provides another example of cyclic curves obtained from existing and proposed numerical models under an STD type loading protocol. Softening branches are not considered in backbone curves for either model. Figure 7a depicts cyclic curves without considering damage rule. This is done by setting α_1 in Eq. (2) to zero. Cyclic and monotonic deterioration is not evident in Fig. 7a. Figure 7b, and c shows the cyclic curves of the existing and the proposed models, respectively. In Fig. 7c, the proposed model can simulate monotonic (in-cyclic) degradation, whereas existing models cannot simulate monotonic degradation. Figures 6b and 7c reveal that the proposed numerical model can simulate monotonic strength degradation under both monotonic and cyclic loads, even if the softening branch is not predefined in the backbone curves. Table 2 summarizes important features of existing and proposed models.

3 Model Parameter Calibration

Model parameters are calibrated based on test data of RC columns to accurately reproduce the measured load–deformation responses. Before calibrating model parameters, the $P-\Delta$ effect is excluded from the test results to establish a pure relationship between force and deformation (Lee and Han 2018; Haselton et al. 2007; Liao et al. 2017). Two sets of model parameters are calibrated: (1) backbone curve parameters, (2) damage parameters.

Backbone curve parameters are calibrated based on the first-cycle envelopes according to FEMA 440 (FEMA 2005). Figure 8a shows a calibrated backbone curve and its constituent modeling parameters. The capping point (θ_c, f_c) is defined as the point corresponding to the maximum strength determined from the measured cyclic envelope. The yield point (θ_y, f_y) is determined using an iterative procedure: (1) assume a point (θ_y, f_y); (2) construct a line connecting the origin and the point on the envelope corresponding to 0.6 f_y according to Sect. 4 of FEMA 440; (3) calculate the difference in areas under the cyclic envelope (A_1 in Fig. 8) and under the idealized backbone curve (A_2 in Fig. 8) up to the capping point; (4)

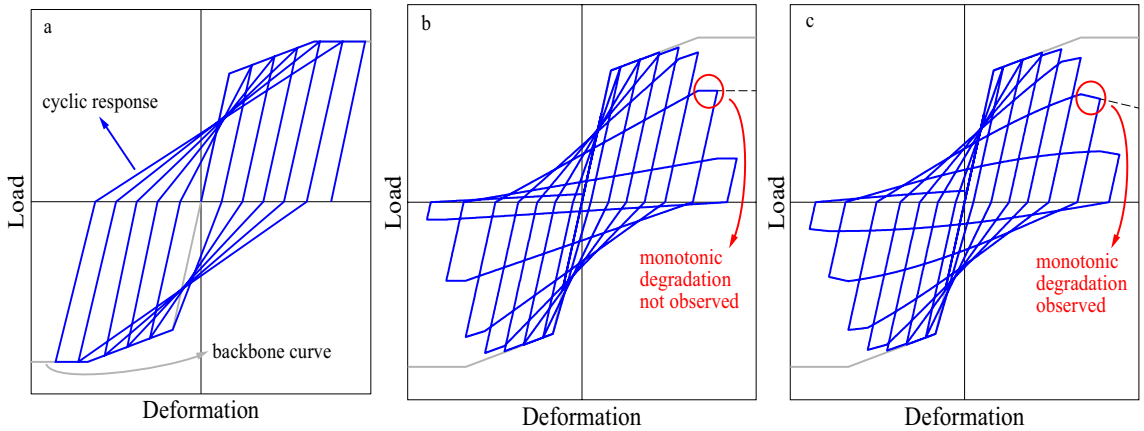

Fig. 7 Cyclic curves obtained from existing and proposed numerical models: **a** model without damage rule, **b** existing model with Eq. (3), **c** proposed model with Eq. (5).

Table 2 Characteristics of existing and proposed numerical models.

	Existing model	Proposed model
Hysteretic rule	Peak-oriented	Peak-oriented
Backbone curve	Tri-linear curve with or without a softening branch	Tri-linear curve without a softening branch
Damage rule	δ is calculated using cumulative energy, and is updated at deformation reversal	δ is calculated using cumulative deformation, and is updated at every analysis step

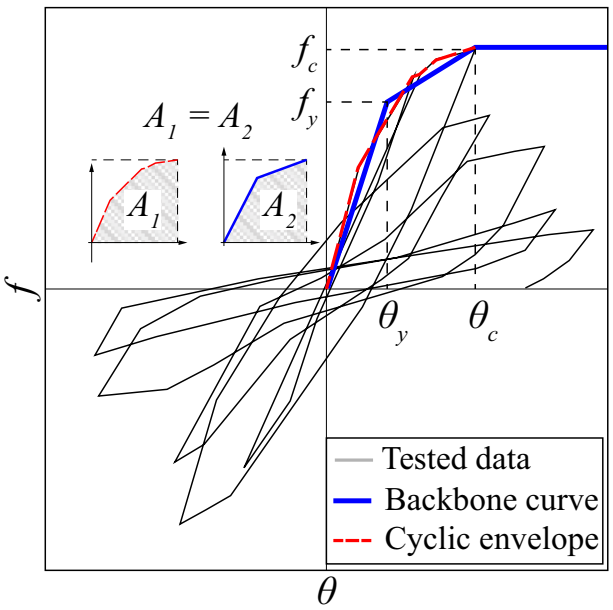

Fig. 8 Backbone curve parameter calibration.

repeat steps (1) to (3) until the specified tolerance of the difference in two areas is satisfied ($\leq 0.1\%$).

Once the idealized backbone curve is constructed, the values of cyclic strength degradation parameters ($\boldsymbol{\alpha}_1$,$\boldsymbol{\alpha}_2$) are determined with respect to the idealized backbone curve. Parameters $\boldsymbol{\alpha}_1$ and $\boldsymbol{\alpha}_2$ that best fit the measured load–deformation responses should be tuned simultaneously. To estimate the $\boldsymbol{\alpha}_1$ and $\boldsymbol{\alpha}_2$ values effectively, the genetic algorithm was used in this study.

4 Validation of the Proposed Hysteretic Model for RC Columns

To verify the proposed numerical model, the cyclic curves of three different sets of column specimens (Table 1) are simulated using the proposed model: (1) set 1, two specimens tested by Sezen and Moehle (2006); (2) set 2, six specimens tested by Takemura and Kawashima (1997); (3) set 3, five specimens tested by Nojavan et al. (2015); and (4) set 4, four specimens tested by Pujol et al. (2006). Although each set contains identical column specimens, specimens in each set were tested under different loading protocols. Because the main feature of the proposed model is the nature of loading-protocol independency, the cyclic curves of column specimens in each set are simulated using the values of modeling parameters determined for the first specimen in the set (specimens S1 for set 1, T1 for set 2, and N1 for set 3). The cyclic curves are also simulated using the existing numerical model provided in Table 2, with the values for the modeling parameters determined for the first specimen in each set and compared with those obtained from the proposed model. The backbone curve without a softening branch is idealized from the first-cycle envelope curves for both numerical models (Fig. 7). Modeling parameters of cyclic degradation are determined to match the measured cyclic degradation.

To evaluate the accuracy of simulation results, the Ω value is calculated using Eq. (6), which is the root mean squared error in the calculated lateral forces ($f_{i,cal}$) at every analysis steps ($i = 1$ to N) with respect to the measured lateral forces ($f_{i,test}$) at corresponding loading steps:

$$\Omega = \sqrt{\frac{\sum_{i=1}^{N} (f_{i,cal} - f_{i,test})^2}{N}} \tag{6}$$

4.1 Set 1: Specimens Tested by Sezen and Moehle (2006)

Figure 9 shows the measured and simulated cyclic curves of specimens S1 and S2 from the proposed and existing numerical models. Cyclic curves are simulated for specimens S1 and S2 with the same loading protocol shown in Fig. 9a-1. For specimen S1, both the existing and proposed models produce cyclic curves accurately (Fig. 9 b-1, c-1). However, it is noted that the cyclic curves simulated from the proposed model does not perfectly match the measured cyclic curves over the entire drift ranges. Particularly, in a drift ratio ranging from 2 to 3%, the discrepancy between simulated and measured cyclic curves is noticeable. Although the proposed model is a simple model, the model needs to be improved in future study.

For specimen S2 (Fig. 9b-2), cyclic curves simulated from the existing model deviates significantly from the measured cyclic curves in the softening branch ($\theta \geq 2\%$). In contrast, the proposed model simulates the softening response accurately, although the values of modeling parameters determined for specimen S1 are used for the simulation. This proves that the proposed model produces consistently accurate load–deformation responses irrespective of loading protocols.

The values of Ω for specimens S1 and S2 are calculated for the proposed and exiting models using Eq. (6) and summarized in Table 3. For specimen S1, the difference in the **Ω** values for the existing and proposed models is only 1%. The error produced by the existing model is slightly smaller than that produced by the proposed model. However, for specimen S2 tested under a loading protocol different from that used for specimen S1, the ***Ω*** value of the proposed model is 25% smaller than that of the exiting model. This indicates that the simulation accuracy of the proposed hysteretic model improves by 25% compared to that of the existing model. This indicates that the proposed model produces small error irrespective of the types of loading protocols.

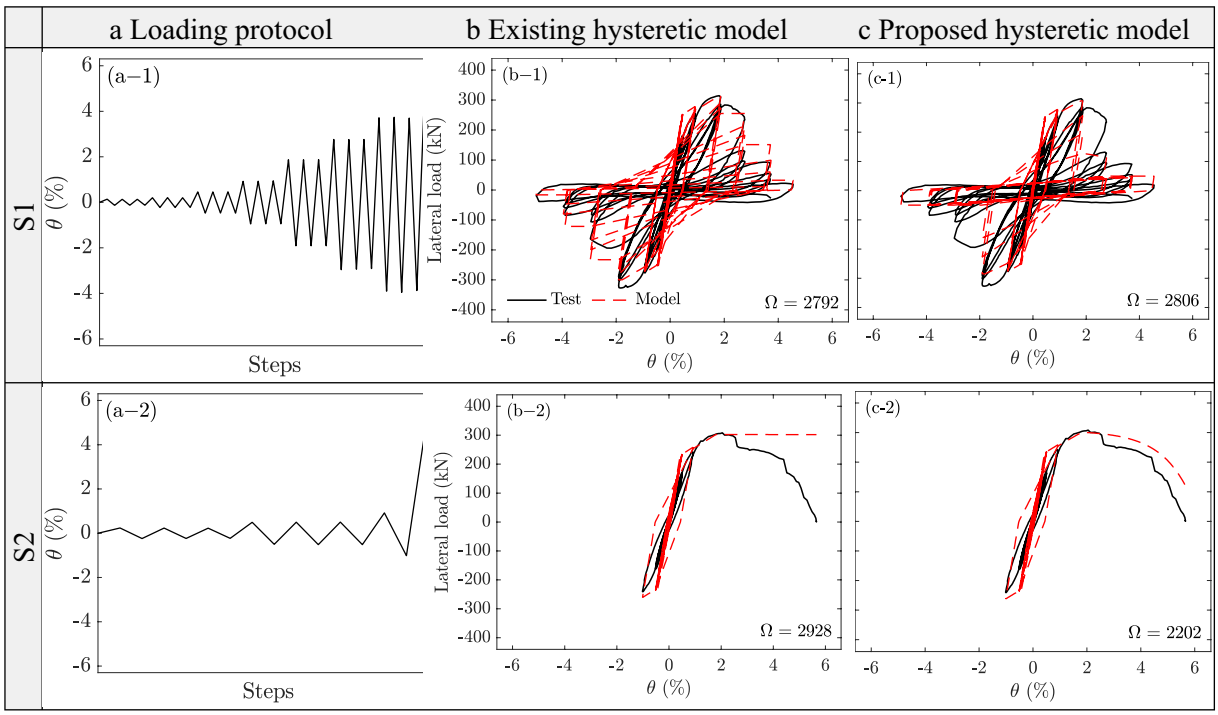

Fig. 9 Measured and simulated cyclic curves of specimens tested by Sezen and Moehle (2006): **a** loading protocol, **b** existing hysteretic model, **c** proposed hysteretic model.

Table 3 Ω values of the existing and proposed models for specimens.

Set	Specimens	Ω (exiting model) (1)	Ω (proposed model) (2)	(2)/(1)
1	S1	2792	2806	1.01
	S2	2928	2202	0.75
2	T1	382	393	1.03
	T2	1025	672	0.66
	T3	728	386	0.53
	T4	1500	223	0.15
	T5	581	575	0.99
	T6	1098	287	0.26
3	N1	104,467	104,459	1.00
	N2	49,480	42,664	0.86
	N3	105,279	104,266	0.99
	N4	133,116	101,100	0.76
	N5	119,043	84,858	0.71
4	P1	349	349	1.00
	P2	321	318	0.99
	P3	286	283	0.99
	P4	243	240	0.99

4.2 Set 2: Specimens Tested by Takemura and Kawashima (1997)

Figure 10 shows cyclic curves of six identical specimens tested with different loading protocols by Takemura and Kawashima (1997) and the simulated cyclic curves using the proposed and existing numerical models. The proposed model generally produces cyclic curves that generally match the measured cyclic curves better than the existing model.

The Ω values of six specimens are calculated for the proposed and existing models using Eq. (6) and summarized in Table 3. The ratios of Ω values of the proposed model to those of the existing model for specimens T1, T2, T3, T4, T5 and T6 are 1.03, 0.66, 0.53, 0.15, 0.99, and 0.26, respectively, indicating that the proposed numerical model simulates the cyclic curves of specimens more accurately than does the exiting model.

4.3 Set 3: Specimens Tested by Nojavan et al. (2015)

Measured and simulated cyclic curves of five identical column specimens tested with different loading protocols by Nojavan et al. (2015) are shown in Fig. 11. Cyclic

(See figure on next page.)

Fig. 10 Measured and simulated cyclic curves of specimens tested by Takemura, Kawashima (1997): **a** loading protocol, **b** existing model, **c** proposed model.

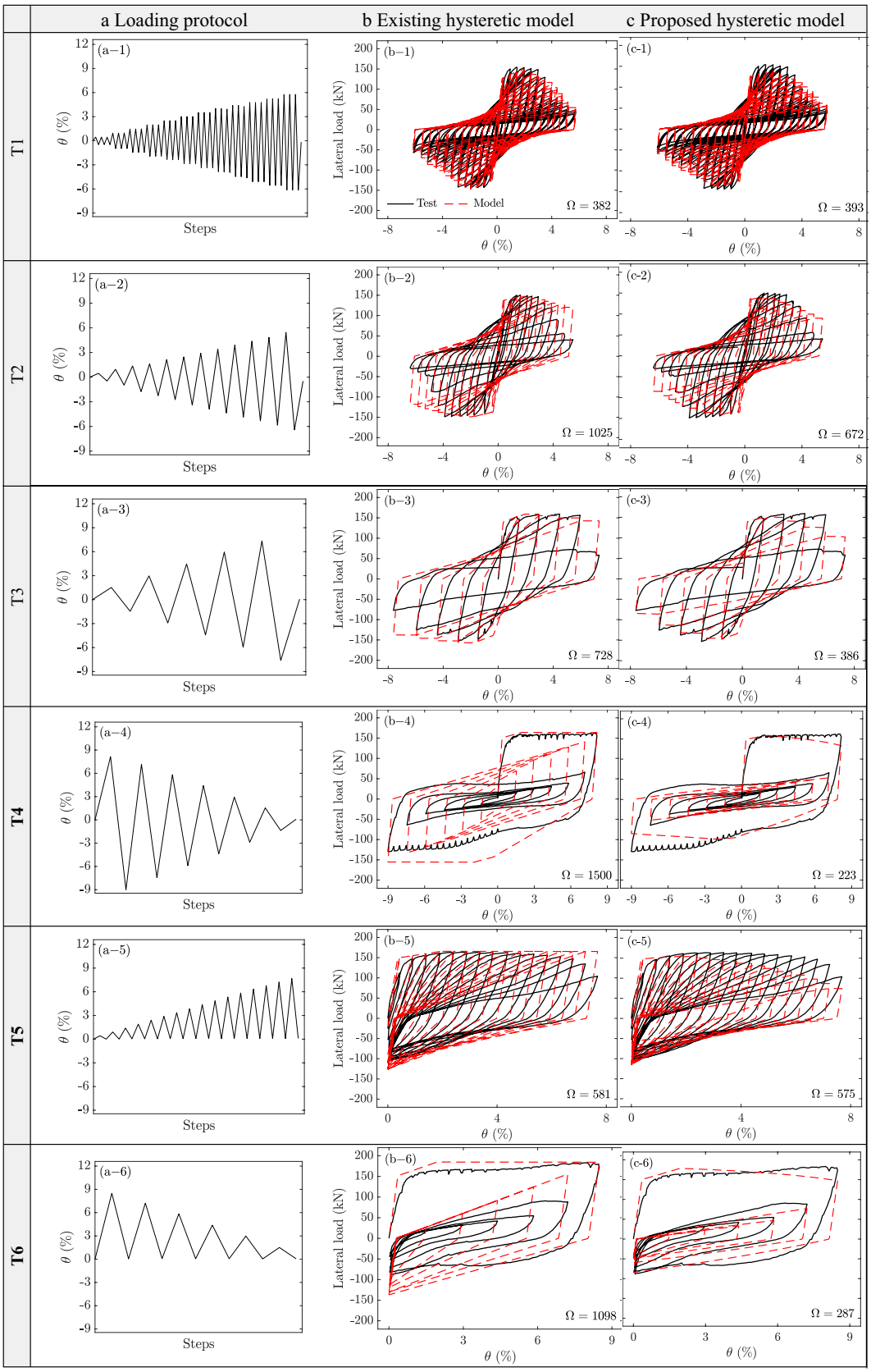
a Loading protocol
b Existing hysteretic model
c Proposed hysteretic model
T1
T2
T3
T4
T5
T6
(a−1)
(a−2)
(a−3)
(a−4)
(a−5)
(a−6)
(b−1)
(b−2)
(b−3)
(b−4)
(b−5)
(b−6)
(c-1)
(c-2)
(c-3)
(c-4)
(c-5)
(c-6)
θ (%)
Steps
Lateral load (kN)
Test
Model
Ω = 382
Ω = 393
Ω = 1025
Ω = 672
Ω = 728
Ω = 386
Ω = 1500
Ω = 223
Ω = 581
Ω = 575
Ω = 1098
Ω = 287

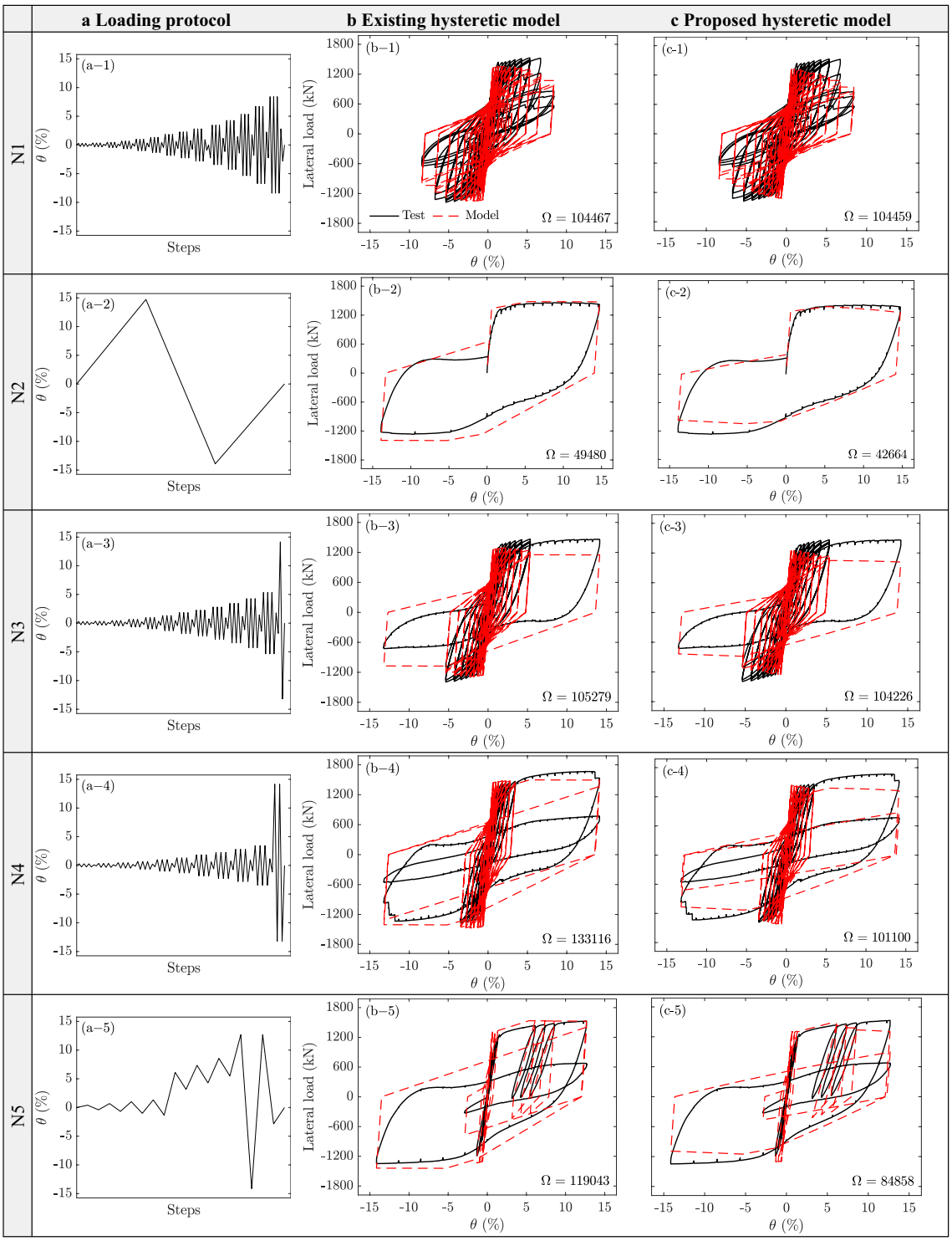

Fig. 11 Measured and simulated cyclic curves of specimens tested by Nojavan et al. (2015): **a** loading protocol, **b** existing hysteretic model, **c** proposed hysteretic model.

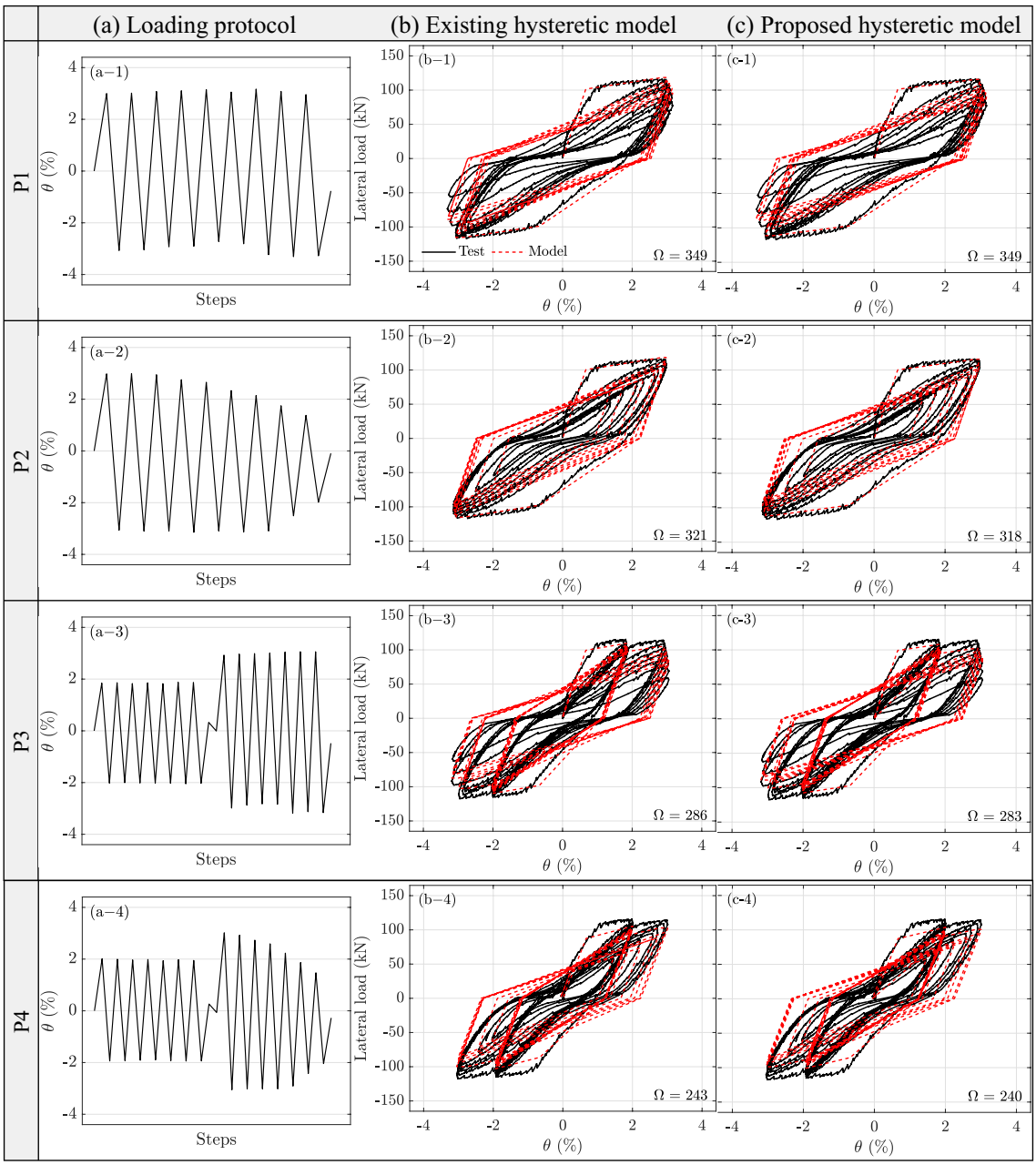

Fig. 12 Measured and simulated cyclic curves of specimens tested by Pujol et al. (2006): **a** loading protocol, **b** existing hysteretic model, **c** proposed hysteretic model.

curves simulated using the proposed model match the measured cyclic curves better than those simulated by the existing model.

The Ω values of the five specimens are calculated using Eq. (6) for the proposed and existing models (Table 3). The respective Ω ratios of the proposed model to those of the existing model for specimens N1, N2, N3, N4, and N5 are 1.00, 0.86, 0.99, 0.76, and 0.71, respectively. The proposed model simulates cyclic curves of specimen N1 with negligible improvement over the existing model. However, it simulates cyclic curves for specimens N2, N3, N4, N5, and N6 more accurately than the existing

model irrespective of loading protocols. The proposed model produces superior simulation results compared with the existing model for specimens N4 and N5, which were tested under a mix of STD and other loading protocols, which is similar to near-collapse loading protocol. Although overall simulation results are improved by using the proposed model compared with those from the existing model, the proposed model needs to be improved to simulate softening branches more accurately.

4.4 Set 4: Specimens Tested by Pujol et al. (2006)

Figure 12 shows cyclic curves of four identical specimens tested by Pujol et al. (2006) with different loading protocols and those simulated from the existing and proposed models.

Unlike observations from the specimens shown in Figs. 9, 10, 11, the difference between cyclic curves simulated with the existing and proposed models is not distinct. The proposed model produces slightly accurate results than the existing model. The Ω value of the proposed model for four specimens is only 1% less than that of the existing model. Such small difference in the Ω value between the two models may have resulted from the loading protocols used in the test. All loading protocols used in the tests were almost symmetric in the positive and negative loading directions. The existing model may produce reasonable simulation results for columns tested under symmetric loading protocols. Another reason is attributed to the fact that those specimens were not tested under large deformation amplitudes developing significant post-capping responses unlike other specimens listed in Table 3. As observed in previous sections, the existing and proposed models produced distinctively different results in the softening branch.

5 Summary and Conclusions

In this study, a numerical model was proposed to simulate the cyclic curves of RC columns and to resolve drawbacks of existing numerical models dependent on loading protocols.

The model implemented the peak-oriented hysteretic rule. Backbone curves were idealized from the first-cycle envelope of measured cyclic curves. Softening branches were not considered to avoid inaccuracies in modeling due to large fluctuations in the softening branch of envelopes according to loading protocols. In the proposed model, the damage variable was updated at every loading step to simulate the softening response associated with both in-cyclic and cyclic degradations.

The model was validated by comparing simulated and measured cyclic curves of four different sets of RC columns specimens. Each set contained identical columns specimens tested under different loading protocols. The values of modeling parameters were determined for the first specimen of each set. The proposed model generally produced cyclic curves of column specimens more accurately than the existing model. To evlauate the accuracy of the proposed model, the (Ω) calue was calculated, which is the root mean squared error in the calcuated lateral force ($f_{i,cal}$) at every analysis steps with respect to the measured lateral forces ($f_{i,test}$) at corresponding loading steps. The Ω value produced by the proposed model was up to 85% smaller than that produced by the existing model. The ratio of the Ω value for the proposed model to that for the existing model ranged from 0.15 to 1.03. When loading history is significantly different from convention fully reversed cyclic loading, the Ω value for the existing model was much greater than that for the proposed model. For convention fully reversed cyclic loading, the difference between the Ω values for the proposed and existing models was minor (< 5%). This indicates that the proposed model simulated hysteretic behavior of RC columns accurately irrespective of loading protocols.

To simulate the cyclic curves of a column without test data, predictive equations are required to calculate the values of constituent model parameters with column dimensions, material properties, reinforcement ratios, etc. It is beyond the scope of this study to propose these equations. But it will be done in a future study. In addition, the proposed model needs to be improved to simulate cyclic curves more accurately in the entire drift ranges.

Acknowledgements
This research was funded by the National Research Foundation of Korea (NRF-2020R1A2C2010548). The valuable comments of three anonymous reviewers are greatly appreciated.

Authors' contributions
The first author, C.S. Lee developed the numerical model. The corresponding author, S.W.Han supervised the project and completed the model and numerical analyses. All authors read and approved the final manuscript.

Authors' information
Chang Seok Lee, Post-Doc. Department of Architectural Engineering, Hanyang University, Seoul 04,763, Korea.

Sang Whan Han, Professor, Department of Architectural Engineering, Hanyang University, Seoul 04,763, Korea.

Funding
The National Research Foundation of Korea Grant Number: (NRF-2020R1A2C2010548).

Availability of data and materials
Not applicable.

Competing interests
Not applicable (no competing interest).

Received: 8 July 2020 Accepted: 12 November 2020
Published online: 14 January 2021

References

ASCE. (2017). *Seismic Evaluation and Retrofit of Existing Buildings*. ASCE 41–17, American Society of Civil Engineers, Reston, VA.
ATC. (2010). *Modeling and acceptance criteria for seismic design and analysis of tall buildings*. ATC 72–1. Applied Technology Council, CA.
Berry, M., Parrish, M., & Eberhard, M. (2004). *PEER Structural Performance database user's manual*. Pacific Earthquake Engineering Research Center: University of California, Berkeley, CA, USA.
Chowdhury, S. R., & Orakcal, K. (2012). An analytical model for reinforced concrete columns with lap splices. *Engineering Structures, 43,* 180–193.
Clough, R.W., Johnston, S.B. (1966). Effect of stiffness degradation on earthquake ductility requirements. *Proceedings of Japan Earthquake Engineering Symposiu*m, Tokyo.
Eads, L., Miranda, E., Krawinkler, H., & Lignos, D. G. (2013). An efficient method for estimating the collapse risk of structures in seismic regions. *Earthquake Engineering and Structural Dyannmics, 42*(1), 25–41.
Elkady, A., & Lignos, D. G. (2014). Modeling of the composite action in fully restrained beam-to-column connections: implications in the seismic design and collapse capacity of steel special moment frames. *Earthquake Engineering and Structural Dyannmics, 43*(13), 1935–1954.
El-Sokkary, H., & Galal, K. (2009). Analytical investigation of the seismic performance of RC frames rehabilitated using different rehabilitation techniques. *Engineering Structures, 31*(9), 1955–1966.
Elwood, K. J., & Moehle, J. P. (2005). Drift capacity of reinforced concrete columns with light transverse reinforcement. *Earthquake Spectra, 21*(1), 71–89.
FEMA P440A. (2009). *Effects of strength and stiffness degradation on seismic response*. FEMA P440A. Department of Homeland Security, Washington, D.C.
FEMA 440. (2005). *Improvement of nonlinear static seismic analysis procedures*. FEMA 440. Federal Emergency Management Agency, Washington, DC.
Galanis, P. H., & Moehle, J. P. (2015). Development of collapse indicators for risk assessment of older-type reinforced concrete buildings. *Earthquake Spectra, 31*(4), 1991–2006.
Ghannoum, W. M., & Moehle, J. R. (2012). Dynamic collapse analysis of a concrete frame sustaining column axial failures. *ACI Structural Journal, 109*(3), 403–412.
Goulet, C. A., Haselton, C. B., Mitrani-Reiser, J., Beck, J. L., Deierlein, G. G., Porter, K. A., & Stewart, J. P. (2007). Evaluation of the seismic performance of a code-conforming reinforced-concrete frame building—from seismic hazard to collapse safety and economic losses. *Earthquake Engineering and Structural Dyannmics, 36*(13), 1973–1997.
Han, S. W., Koh, H., & Lee, C. S. (2019). Accurate and efficient simulation of cyclic behavior of diagonally reinforced concrete coupling beams. *Earthquake Spectra, 35*(1), 361–381.
Han, S. W., Kwon, O.-S., & Lee, L.-H. (2004). Evaluation of the seismic performance of a three-story ordinary moment-resisting concrete frame. *Earthquake engineering and structural dyannmics, 33*(6), 669–685.
Haselton, C. B., Liel, A. B., Deierlein, G. G., Dean, B. S., & Chou, J. H. (2011). Seismic collapse safety of reinforced concrete buildings i: assessment of ductile moment frames. *Journal of Structural Engineering, ASCE, 137*(4), 481–491.
Haselton, C.B., Liel, A.B., Lange, S.T., Deierlein, G.G. (2007). *Beam-Column Element Model Calibrated for Predicting Flexural Response Leading to Global Collapse of RC Frame Buildings.* PEER Report 2007/03. University of California, Berkeley, Pacific Earthquake Engineering Research Center.
Ibarra, L. F., Medina, R. A., & Krawinkler, H. (2005). Hysteretic models that incorporate strength and stiffness deterioration. *Earthquake Engineering and Structural Dyannmics, 34*(12), 1489–1511.
Krajcinovic, D. (1983). Constitutive equations for damaging materials. *Journal of Applied Mechanics, 50*(2), 355–360.
Krawinkler, H.(2009). Loading histories for cyclic tests in support of performance assessment of structural components. *Proceeding of the 3rd International Conference on Advances in Experimental Structural Engineering (3AESE),* San Francisco, CA.
LeBorgne, M. R., & Ghannoum, W. M. (2014a). Calibrated analytical element for lateral-strength degradation of reinforced concrete columns. *Engineering Structures, 81,* 35–48.
Lee, C. S., & Han, S. W. (2018). Computationally effective and accurate simulation of cyclic behaviour of old reinforced concrete columns. *Engineering Structures, 173,* 892–907.
Li, Y., & Sanada, Y. (2017). Seismic strengthening of existing RC beam-column joints by wing walls. *Earthquake Engineering and Structural Dyannmics, 46*(12), 1987–2008.
Liao, W.-C., Perceka, W., & Wang, M. (2017). Experimental study of cyclic behavior of high-strength reinforced concrete columns with different transverse reinforcement detailing configurations. *Engineering Structures, 153,* 290–301.
Liel, A. B., Haselton, C. B., & Deierlein, G. G. (2011). Seismic collapse safety of reinforced concrete buildings. II: comparative assessment of nonductile and ductile moment frames. *Journal of Structural Engineering, ASCE, 37*(4), 492–502.
Lignos, D. G., Hikino, T., Matsuoka, Y., & Nakashima, M. (2013). Collapse assessment of steel moment frames based on e-defense full-scale shake table collapse tests. *Journal of structural engineering, ASCE, 139*(1), 120–132.
Lignos, D. G., & Krawinkler, H. (2011). Deterioration modeling of steel components in support of collapse prediction of steel moment frames under earthquake loading. *Journal of Structural Engineering, ASCE, 137*(11), 1291–1302.
Lignos, D. G., Putman, C., & Krawinkler, H. (2015). Application of simplified analysis procedures for performance-based earthquake evaluation of steel special moment frames. *Earthquake Spectra, 31*(4), 1949–1968.
LeBorgne, M.R., Ghannoum, W. M. (2014). Analytical Element for Simulating Lateral-Strength Degradation in Reinforced Concrete Columns and Other Frame Members. *Journal of structural engineering*, ASCE, 140(7), 04014038 04014031–04014012.
Lowes, L.N., Altoontash, A.(2003). Modeling reinforced-concrete beam-column joints subjected to cyclic loading. *Journal of structural engineering* ASCE, 129(12), 1686–1697.
Lynn, A. C., Moehle, J. P., Mahin, S. A., & Holmes, W. T. (1996). Seismic evaluation of existing reinforced concrete building columns. *Earthquake Spectra, 12*(4), 715–739.
Maison, B. F., & Speicher, M. S. (2016). Loading protocols for ASCE 41 backbone curves. *Earthquake Spectra., 32*(4), 2513–2532.
Mahin, S. A., & Bertero, V. V. (1976). Nonlinear seismic response of a coupled wall system. *Journal of Structure Division, ASCE, 102*(9), 1759–1780.
Moon, K. H., Han, S. W., & Lee, C. S. (2017). Seismic retrofit design method using friction damping systems for old low- and mid-rise regular reinforced concrete buildings. *Enginering Structures, 146,* 105–117.
NIST. (2010). *Nonlinear structural analysis for seismic design*. NIST GCR 10–917–5, vol. National Institute of Standards and Technology, Gaithersburg, MD.
Nojavan, A., Schultz, A. E., Haselton, C., Simathathien, S., Liu, X., & Chao, S.-H. (2015). A new data set for full-scale reinforced concrete columns under collapse-consistent loading protocols. *Earthquake Spectra, 31*(2), 1211–1231.
Park, Y. J., & Ang, A. H. S. (1985). Mechanistic seismic damage model for reinforced concrete. *Journal of Structural Engineering, ASCE, 111*(4), 722–739.
Park, R., Paulay, T.(1975) *Reinforced Concrete Structures*. John Wiley & Sons, Inc.
PEER. (2017). *Guidelines for performance-based seismic design of tall buildings, version 2.03*. CA: Pacific Earthquake Engineering Center.
Pujol, S., Sozen, M. A., & Ramirez, J. A. (2006). Displacement history effects on drift capacity of reinforced concrete columns. *ACI Materials Journal, 103*(2), 253–262.
Ronagh, H. R., & Baji, H. (2014). On the FE modeling of frp-retrofitted beam-column subassemblies. *International Journal of Concrete Structures and Materials, 8,* 141–155.
Sae-Long, W., Limkatanyu, S., Prachasaree, W., Horpibulsuk, S., & Panedpojaman, P. (2019). Nonlinear frame element with shear-flexure interaction for seismic analysis of non-ductile reinforced concrete columns. *International Journal of Conmcrete Structure and Materials, 13,* 1–19.

Sezen, H., & Chowdhury, T. (2009). Hysteretic model for reinforced concrete columns including the effect of shear and axial load failure. *Journal of Structural Engineering, ASCE, 135*(2), 139–146.
Sezen, H., & Moehle, J. R. (2006). Seismic tests of concrete columns with light transverse reinforcement. *ACI Structural Journal, 103*(6), 842–849.
Takemura, H., & Kawashima, K. (1997). Effect of hysteresis on ductility capacity of reinforced concrete bridge piers. *Journal of Structural Engineering (JSCE), 43A,* 849–858.
Tothong, P., & Luco, N. (2007). Probabilistic seismic demand analysis using advanced ground motion intensity measures. *Earthquake Enigneering and Structural Dynamics, 36*(13), 1837–1860.
Wen, Y. K., Collins, K. R., Han, S. W., & Elwood, K. J. (1996). Dual-level designs of buildings under seismic loads. *Structural Safety, 18*(2–3), 195–224.
Yue, J., Qian, J., & Beskos, D. E. (2016). A generalized multi-level seismic damage model for RC framed structures. *Soil Dynamics and Earthquake Engineering, 80,* 25–39.

Publisher's Note